

# Perturbative evolution at small $x$

P V Landshoff  
DAMTP, University of Cambridge

October 23, 2018

## Abstract

The conventional approach to perturbative evolution is illegal because the expansion in powers of  $\alpha_s$  of the the DGLAP splitting matrix  $\mathbf{P}(\mathbf{z}, \alpha_s)$  breaks down at small  $z$ . The small- $x$  data for the proton structure function  $F_2(x, Q^2)$  and its charm component  $F_2^c(x, Q^2)$  show that a hard pomeron, with intercept close to 1.4, must be added to the familiar soft pomeron. Conventional perturbative evolution may be applied to the hard-pomeron component and provides a striking test of perturbative QCD.

## 1 Introduction

A striking discovery at HERA has been the rapid rise of  $\sigma^{\gamma^* p}$  with  $W^2$  at even quite small fixed values of  $Q^2$ : see figure 1. If one parametrises the rise as an effective power

$$\sigma(\gamma^* p) \sim F(Q^2) (W^2)^{\lambda(Q^2)} \quad (1)$$

then the power  $\lambda(Q^2)$  is found to be significantly greater than the value 0.08 that is familiar in purely hadronic collisions[1]. The value of  $\lambda(Q^2)$  has been extracted[3] by the H1 collaboration from their data and is shown in figure 2, from which it can be seen to increase with  $Q^2$  and reach about 0.4 at the highest values that have been measured.

When  $W^2 \gg Q^2$ ,  $x$  is small and  $W^2 \sim Q^2/x$ . Then the effective-power behaviour (1) corresponds to

$$F_2(x, Q^2) \sim f(Q^2) x^{-\lambda(Q^2)} \quad (2)$$

When they extracted  $\lambda(Q^2)$  from their data, to make the plot of figure 2, H1 assumed that the value of  $\lambda(Q^2)$  at small  $x$  is independent of  $x$  at each  $Q^2$ . While the data are compatible with this assumption, they do not require it and it does not have theoretical justification. Rather, one should parametrise the data with a sum of fixed powers of  $x$ , whose relative weight varies with  $Q^2$ . In the two-pomeron model I will describe, the resulting  $\lambda(Q^2)$  has significant variation with  $x$ , as is seen in figure 3.

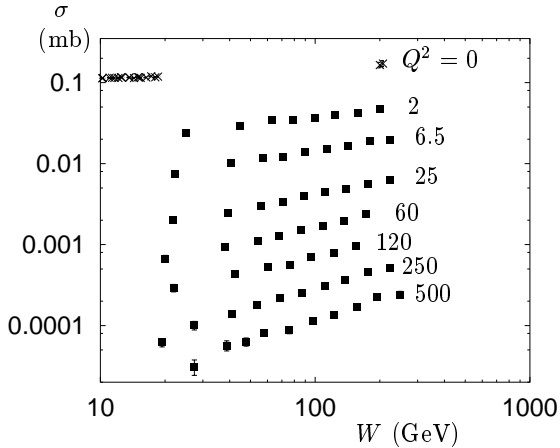


Figure 1: Data[2] for  $\sigma^{\gamma^* p} = (4\pi^2 \alpha_{\text{EM}}/Q^2) F_2$  at various values of  $Q^2$ , together with real-photon data

Even before the HERA measurements, there were predictions[4, 5] that  $\lambda(Q^2)$  would be large at high values of  $Q^2$ . Such predictions arose from two different equations of perturbative QCD: the DGLAP equation and the BFKL equation. However, it has since been realised that the predictions are not as clean as initially had been hoped.

The BFKL equation is applicable when  $x$  is small, and  $Q^2$  large but not too large. It can be made to give values of  $\lambda(Q^2)$  close to  $\frac{1}{2}$ , which is approximately what experiment finds at high  $Q^2$ . This led to talk of a second pomeron, the hard pomeron, with a  $\lambda(Q^2)$  that might be calculated from perturbative QCD. However, it has been realised that this calculation is almost certainly invalid. Apart from concerns that the approximations used to derive the BFKL equation do not take sufficient account of energy conservation[6], it is not correct to suppose that the equation enables  $\lambda(Q^2)$  to be calculated from perturbative QCD alone[7]. While it is conceivable[8, 9] that there is no such problem with purely-hard processes such as  $\gamma^* \gamma^*$  collisions at very high  $Q^2$ , for semi-hard collisions such as  $\gamma^* p$  the BFKL equation inevitably receives important contributions from uncalculable nonperturbative effects.

The DGLAP equation is derived from perturbative QCD and therefore is valid at sufficiently large  $Q^2$ . It couples the  $Q^2$  variation of the quark distributions in the proton to the gluon distribution. When  $Q^2$  is much larger than all the relevant quark masses, the gluon distribution affects the  $Q^2$  variation of all the quark and antiquark distributions equally, and the  $Q^2$  variation of the gluon distribution itself receives equal contributions from all the quark and antiquark distributions. That is, the gluon distribution's evolution is coupled to the singlet

quark distribution, which is the sum of the quark and antiquark distributions:

$$q(x, Q^2) = u + \bar{u} + d + \bar{d} + c + \bar{c} + s + \bar{s} + \dots \quad (3)$$

The number of heavy-quark terms that should be included depends on the value of  $W$ . So the relevant form of the DGLAP equation introduces the two-component quantity

$$\mathbf{u}(x, Q^2) = \begin{pmatrix} q(x, Q^2) \\ g(x, Q^2) \end{pmatrix}. \quad (4)$$

It reads

$$Q^2 \frac{\partial}{\partial Q^2} \mathbf{u}(x, Q^2) = \int_x^1 dz \mathbf{P}(z, \alpha_s(Q^2)) \mathbf{u}(x/z, Q^2). \quad (5)$$

Here,  $\mathbf{P}(z, \alpha_s(Q^2))$  is a  $2 \times 2$  matrix, called the splitting matrix. The DGLAP equation becomes very simple if we introduce the Mellin transforms of  $\mathbf{u}(x, Q^2)$  and  $\mathbf{P}(z, \alpha_s(Q^2))$

$$\mathbf{u}(N, Q^2) = \int_0^1 dx x^{N-1} \mathbf{u}(x, Q^2) \quad (6)$$

and

$$\mathbf{P}(N, \alpha_s(Q^2)) = \int_0^1 dz z^N \mathbf{P}(z, \alpha_s(Q^2)). \quad (7)$$

Then

$$\frac{\partial}{\partial t} \mathbf{u}(N, Q^2) = \mathbf{P}(N, \alpha_s(Q^2)) \mathbf{u}(N, Q^2). \quad (8)$$

In order to apply the DGLAP equation, one should first choose some starting value  $Q_0^2$  of  $Q^2$  and fit the parton distributions there to experimental data, as functions of  $x$ . These functions cannot be calculated from perturbative QCD, but the DGLAP equation, together with assumptions about the form of the gluon distribution, determines how they change as  $Q^2$  increases. If[10] one starts at some fairly small value  $Q_0^2$  of  $Q^2$  with parton distributions that are rather flat in  $x$  at small  $x$ , then an application of the DGLAP equation results in distributions that rapidly become steeper as  $Q^2$  increases, in good agreement with experiment[11, 12]. However, this application is controversial. It is not safe to apply a perturbative equation for choices of  $Q_0^2$  as small as 1 GeV<sup>2</sup> or less, as is sometimes done. Indeed, it is necessary at present to expand the splitting matrix  $\mathbf{P}(z, \alpha_s(Q^2))$  in powers of  $\alpha_s$  and this is unsafe when  $x$  is small, as I explain below.

## 2 Regge approach

A powerful approach to the small- $x$  data for  $F_2(x, Q^2)$  is to extend the Regge phenomenology that is so successful for soft hadronic processes[13, 1]. Regge theory is not supposed to be a competitor with perturbative QCD, but to co-exist with it, and to be applicable when  $W^2$  is much greater than all the other variables, in particular when it is much greater than  $Q^2$ . When  $x$  is small

$W^2 \sim Q^2/x$ , so the condition that  $W^2 \gg Q^2$  is just that  $x \ll 1$ , however large  $Q^2$  may be.

Regge theory relates high-energy behaviour to singularities in the complex angular momentum plane[14]. For deep inelastic scattering, the complex angular momentum  $l$  is essentially the Mellin-transform  $N$  of (6). The correspondence is

$$N \leftrightarrow l - 1 \quad (9)$$

so that this assumption is equivalent to assuming that the relevant singularities in the complex  $N$ -plane are simple poles. The assumption may be not literally correct, but it turns out to give an excellent description of the small- $x$  data[15]. A pole at  $N = \epsilon$  contributes a power  $x^\epsilon$  to the small- $x$  behaviour of  $F_2$ . So the soft pomeron contributes  $x^{-\epsilon_1}$  with  $\epsilon_1 = 0.08$ . But this is not sufficient to describe the rapid rise with  $1/x$  seen in the data at small  $x$  and large  $Q^2$ . Another term  $x^{-\epsilon_0}$  is needed, with  $\epsilon_0 \approx 0.4$ . We call this  $N$ -plane or  $l$ -plane singularity the hard pomeron. This does not explain what is its dynamical origin: maybe it is perturbative QCD though, as I have explained, initial hopes that it might be derived from the BFKL equation now seem unlikely to be realised.

So the simplest fit to the small- $x$  data corresponds to

$$F_2(x, Q^2) \sim \sum_{i=0,1} f_i(Q^2) x^{-\epsilon_i}. \quad (10)$$

where the  $i = 0$  term is hard-pomeron exchange and  $i = 1$  is soft-pomeron exchange. Regge theory gives no information about the form of the coefficient functions  $f_i(Q^2)$ , beyond that they are analytic functions. Also, because the real-photon cross section is

$$\sigma^{\gamma p} = \frac{4\pi^2 \alpha}{Q^2} F_2 \Big|_{Q^2=0}, \quad (11)$$

at fixed  $W$  the function  $F_2$  vanishes linearly with  $Q^2$  at  $Q^2 = 0$ . If we assume that each term in (10) has this property, then

$$f_i(Q^2) \sim (Q^2)^{1+\epsilon_i} \quad i = 0, 1 \quad (12)$$

near  $Q^2 = 0$ . One might hope that perturbative QCD will determine how the two coefficient functions behave at high  $Q^2$ , but as I will explain so far the theoretical difficulties allow this only for the hard-pomeron coefficient function  $f_0(Q^2)$ . Figure 4 shows[16] how  $f_0$  and  $f_1$  vary with  $Q^2$  if we fit (10) to the data at each  $Q^2$ , including values of  $x$  up to 0.02. This provides a guide on the likely functional forms of the coefficient functions. The  $f_i(Q^2)$  can then be parametrised with suitable functions, whose shapes resemble the data points in the plots and which include a number of parameters. These parameters, and the power  $\epsilon_0$ , may then be varied[16] so as to give the best fit to all the small- $x$  data for  $F_2(x, Q^2)$  together with the data for  $\sigma^{\gamma p}$ . This results in the value

$$\epsilon_0 = 0.437. \quad (13)$$

with

$$f_0(Q^2) = 0.0015 \frac{(Q^2)^{1+\epsilon_0}}{(1+Q^2/9.11)^{1+\frac{1}{2}\epsilon_0}} \quad (14)$$

and

$$f_1(Q^2) = 0.60 \left( \frac{Q^2}{1+Q^2/0.59} \right)^{1+\epsilon_1}. \quad (15)$$

The fit was made[16] imposing  $\epsilon_1 = 0.08$  and using only data with  $x < 0.001$  and therefore  $Q^2 \leq 35$  GeV $^2$ ; see figure 5. With the addition of a term from  $(f_2, a_2)$  exchange, and including also powers of  $(1-x)$  in each term to make the structure function vanish suitably as  $x \rightarrow 1$ , the fit agrees[16] remarkably well with data at larger  $x$ , up to  $Q^2 = 5000$  GeV $^2$ .

Having concluded that the data for  $F_2$  require a hard-pomeron component, it is necessary to test this with other data. The hard pomeron is seen clearly in the charm component of  $F_2$ . This describes events in which a  $D^*$  particle is produced, which are used to extract the contribution  $F_2^c(x, Q^2)$  to the complete  $F_2(x, Q^2)$  from events where the  $\gamma^*$  is absorbed by a charmed quark. The data[18] for  $F_2^c(x, Q^2)$  must be treated with some caution because the experimentalists have to make a very large extrapolation to compensate for limited acceptance. Nevertheless the data have the striking property that, over a wide range of  $Q^2$ , they behave as a fixed power of  $x$ :

$$F_2^c(x, Q^2) = f_c(Q^2)x^{-\epsilon_0} \quad (16)$$

with  $\epsilon_0 \approx 0.4$ : see figure 6. It seems, therefore, that  $F_2^c(x, Q^2)$  at small  $x$  receives a contribution from the hard pomeron and that the soft-pomeron contribution to it is negligibly small. To a very good approximation the hard pomeron seems to be flavour-blind[16]:  $F_2^c(x, Q^2)$  is close to  $\frac{2}{5}$  the hard-pomeron part of  $F_2(x, Q^2)$ . For the ranges of  $x$  and  $Q^2$  where they overlap, the two-pomeron fit and conventional fits based on two-loop unresummed perturbative QCD agree with the data equally well. However, they no longer agree when they are extrapolated to smaller values of  $x$ , as is seen in figure 7.

### 3 Real photons: a crucial question

Because the data of figure 5 include a point at extremely low  $Q^2$ , it should be reliable to extrapolate these data to  $Q^2 = 0$ . This extrapolation is the upper curve shown in figure 8 and, at  $\sqrt{s} = 200$  GeV, the hard-pomeron component contributes about 20  $\mu\text{b}$ . That is, at this energy, the fits with and without a hard-pomeron component differ by about 10%. The errors shown on the data in figure 5 are purely statistical; there is an additional systematic error of about 10% at the lowest  $Q^2$ . So at present it is not possible to decide whether the hard pomeron is present in the  $\sigma^{\gamma p}$  data, though it seems likely.

There is also uncertainty with the data for  $\sigma^{\gamma\gamma}$  from LEP. The cross sections are rather sensitive to the Monte Carlo model used for the unfolding of detector effects, different Monte Carlos producing different results. In figure 9 the resulting uncertainty is contained in the errors on the OPAL data. The L3 data are shown with the use of two Monte Carlos, the errors corresponding to the statistical and systematic errors combined in quadrature. The figure shows the prediction obtained by applying factorisation to  $\sigma^{\gamma p}$  and  $\sigma^{pp}$  data, with no hard-pomeron component. The data from L3, particularly the upper set, may require such a component. and the figure also shows how adding it in might change the fit.

This is an important question. Is the hard pomeron already present at  $Q^2 = 0$ , or is it rather generated by perturbative evolution? If it is there already at  $Q^2 = 0$  it presumably arises because the photon has a pointlike component, as if it is present in the  $\bar{p}p$  total cross section it is very small. Maybe it will be significant at LHC energies.

## 4 Perturbative evolution

I now show that perturbative evolution governs how the hard pomeron's contribution to the structure function increases with  $Q^2$ . It is found[19] that the parametrisation of the hard-pomeron coefficient function  $f_0(Q^2)$  of (10) agrees very well with what is obtained from DGLAP evolution, over a large range of  $Q^2$ . As yet, we are not able to apply perturbative evolution to the soft pomeron.

A power contribution  $f(Q^2)x^{-\epsilon_0}$  to  $F_2(x, Q^2)$  corresponds to a pole

$$\frac{\mathbf{f}(Q^2)}{N - \epsilon_0} \quad \mathbf{f}(Q^2) = \begin{pmatrix} f_q(Q^2) \\ f_g(Q^2) \end{pmatrix} \quad (17)$$

in  $\mathbf{u}(N, Q^2)$ . With four active quark flavours and a flavour-blind hard pomeron,  $f_q(Q^2) = \frac{18}{5}f_0(Q^2)$ . We find[20], on taking the residue of the pole at  $N = \epsilon_0$  on each side of the Mellin transform (8) of the DGLAP equation,

$$\frac{\partial}{\partial t} \mathbf{f}(Q^2) = \mathbf{P}(N = \epsilon_0, \alpha_s(Q^2)) \mathbf{f}(Q^2) \quad (18)$$

If we include four flavours of quark and antiquark in the sum in (3), then at  $Q^2 = 20$  GeV $^2$  the singlet quark distribution  $x \sum_f (q_f + \bar{q}_f) \sim 0.095x^{-\epsilon_0}$  at sufficiently small  $x$ . According to figure 6, the charmed-quark component  $F_2^c$  of  $F_2$  is governed almost entirely by hard-pomeron exchange at small  $x$ , even at small values of  $Q^2$ , and, within the experimental errors, its magnitude is consistent with the hard pomeron being flavour-blind. According to perturbative QCD, the charmed quark originates from a gluon in the proton, and[21] the two distributions are proportional to each other to a good approximation over a wide range of  $x$  and  $Q^2$ . This implies that the gluon distribution also

is hard-pomeron dominated. At  $Q^2=20$  GeV $^2$  and  $x = 0.01$ , a next-to-leading-order fit[22, 23] to the combined ZEUS and H1 data gives  $xg(x, Q^2) = 5.7 \pm 0.7$ . Other authors[24, 25, 26] find much the same value. This is  $8 \pm 1$  times the hard-pomeron component of the singlet quark distribution.

An unresummed perturbation expansion of the splitting matrix  $\mathbf{P}(N, \alpha_s)$  is not valid[20] for small values of  $N$ , but we need  $\mathbf{P}(N, \alpha_s)$  at  $N = 0.437$ , that is far from 0, and so it is reasonable to hope that resummation is not needed. The numerical values of the elements of the splitting matrix  $\mathbf{P}(N, \alpha_s)$  are known[5] in one and two-loop order, so it is straightforward to integrate (18). At the energies being considered it is necessary to use four flavours throughout as the charm contribution is active. The beauty contribution is so small that its omission has a negligible effect.

The result of integrating the differential equation (18) for the singlet quark distribution is shown in figure 10, where the solid curve is the result of the two-loop-order perturbative QCD evolution according to (18), and the broken curve is the Regge fit to the data I have described. The ratio of the gluon distribution to the hard-pomeron component of the singlet quark distribution is taken to be 8.0 at  $Q^2 = 20$  GeV $^2$ . Figure 10 also shows how the gluon distribution

$$xg(x, Q^2) = f_g(Q^2)x^{-\epsilon_0} \quad (19)$$

evolves. Provided one chooses  $\Lambda$  such that  $\alpha_s(M_z^2) = 0.116$ , which is the HERA value[22, 23], there is little difference between the leading-order and next-to-leading-order results.

The conventional approach to evolution expands the splitting matrix  $\mathbf{P}(N, \alpha_s)$  in powers of  $\alpha_s$ . Because an unresummed expansion that needs the splitting matrix at small  $N$  makes the splitting function larger than it really is, a gluon distribution of a given magnitude apparently gives stronger evolution than it really should. That is, the conventional approach will tend to under-estimate the magnitude of  $xg(x, Q^2)$  in certain regions of  $(x, Q^2)$  space. This is verified by the results for the evolution of  $xg(x, Q^2)$  obtained from integrating (18). Figure 11 shows the proton's gluon structure function at two values of  $Q^2$ , according to the solution of (18), which does not use the splitting matrix at small  $N$ , and compares it with what is extracted from the data by conventional means.

The agreement between the extraction of the hard-pomeron component of  $F_2(x, Q^2)$  from experiment, and its calculated evolution, is a striking success both of the hard-pomeron concept and of perturbative QCD. We cannot apply a similar analysis to the soft pomeron, because this would need the splitting matrix  $\mathbf{P}(N, \alpha_s)$  at  $N = 0.08$ , which is too small for an expansion in powers of  $\alpha_s$  to be meaningful. We do not yet know how to perform the necessary resummation[29, 30, 31].

A fuller account of pomeron physics and QCD may be found in a book[32] to be published later this year by Cambridge University Press.

*This research is supported in part by the EU Programme “Training and Mobility of Researchers”, Network “Quantum Chromodynamics and the Deep Structure of Elementary Particles” (contract FMRX-CT98-0194), and by PPARC*

## References

- [1] A Donnachie and P V Landshoff, Physics Letters **B296** (1992) 227
- [2] C Adloff *et al*, **H1** Collaboration, European Physical Journal **C19** (2001) 269
- [3] C Adloff *et al*, **H1** Collaboration, Physics Letters **B520** (2001) 183
- [4] J R Forshaw and D A Ross, *Quantum Chromodynamics and the Pomeron* Cambridge University Press (1997)
- [5] R K Ellis, W J Stirling and B R Webber, *QCD and Collider Physics* Cambridge University Press (1996)
- [6] J C Collins and P V Landshoff, Physics Letters **B276** (1992) 196
- [7] J Bartels, H Lotter and M Vogt, Physics Letters **B373** (1996) 215
- [8] J Bartels, A De Roeck and H Lotter, Physics Letters **B389** (1996) 742
- [9] J Brodsky, F Hautmann and D E Soper, Physical Review **D56** (1997) 6957
- [10] M Glück, E Reya and A Vogt, European Physical Journal **C5** (1998) 461
- [11] A D Martin *et al*, European Physical Journal **C4** (1998) 463
- [12] H L Lai *et al*, Physical Review **D55** (1997) 1280
- [13] A Donnachie and P V Landshoff, Nuclear Physics **B267** (1986) 690
- [14] P D B Collins, *An Introduction to Regge Theory* Cambridge University Press (1977)
- [15] A Donnachie and P V Landshoff, Physics Letters **B437** (1998) 408
- [16] A Donnachie and P V Landshoff, Physics Letters **B518** (2001) 63
- [17] G Altarelli, R D Ball and S Forte, hep-ph/0104246 (2001)
- [18] J Breitweg *et al*, **ZEUS** Collaboration, European Physical Journal **C12** (2000) 35
- [19] A Donnachie and P V Landshoff, hep-ph/0111427 (2001)
- [20] J R Cudell, A Donnachie and P V Landshoff, Physics Letters **B448** (1999) 281

- [21] Z Sullivan and P M Nadolsky, hep-ph/0111358 (2001)
- [22] C Adloff *et al*, **H1** Collaboration, European Physical Journal **C21** (2001) 33
- [23] A Cooper-Sarkar, in *International Europhysics Conference on High Energy Physics Budapest 2001*, D Horvath, P Levai and A Patkos, eds, JHEP (<http://jhep.sissa.it/>) Proceedings Section PrHEP-hep2001/009 (2001)
- [24] A D Martin *et al*, European Physics Journal **C18** (2000) 117
- [25] A D Martin *et al*, hep-ph/0110215 (2001)
- [26] H L Lai *et al*, European Physics Journal **C12** (2000) 375
- [27] Durham data base, [cpt19.dur.ac.uk/hepdata/pdf3.html](http://cpt19.dur.ac.uk/hepdata/pdf3.html)
- [28] C Adloff *et al*, **H1** Collaboration, European Physical Journal **C21** (2001) 33
- [29] M Ciafaloni, D Colferai and G P Salam, Journal of High Energy Physics **0007** (2000) 054
- [30] G Altarelli, R D Ball and S Forte, Nuclear Physics **B599** (2001) 383
- [31] R S Thorne, Physical Review **D64** (2001) 074005
- [32] A Donnachie, H G Dosch, P V Landshoff and O Nachtmann, *Pomeron Physics and QCD* Cambridge University Press (2002)

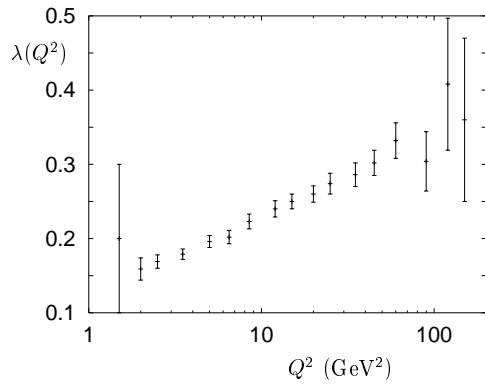


Figure 2: The effective power  $\lambda(Q^2)$  of(1) extracted from H1 data[3]

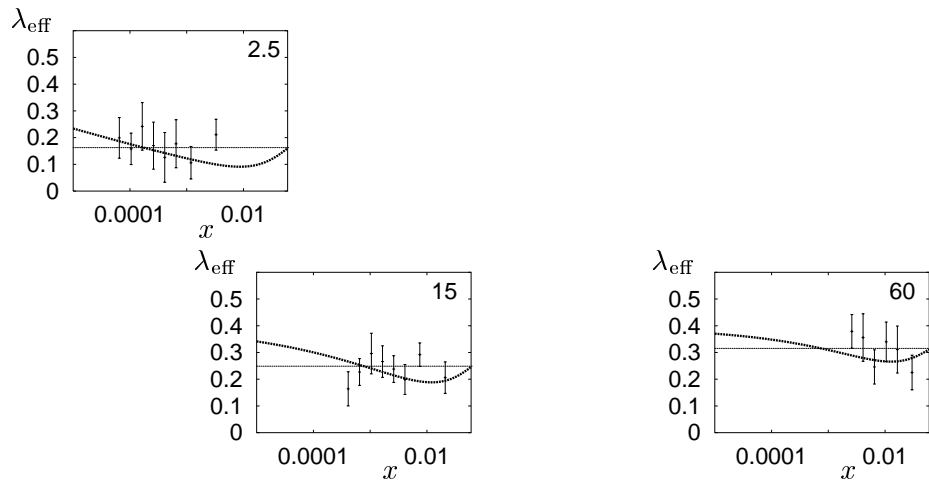


Figure 3: Data[3] for the effective power of  $1/x$  at  $Q^2 = 2.5, 15$  and  $60$  GeV $^2$ . The horizontal lines correspond to the values plotted in figure 2 and the solid lines to the two-pomeron fit.

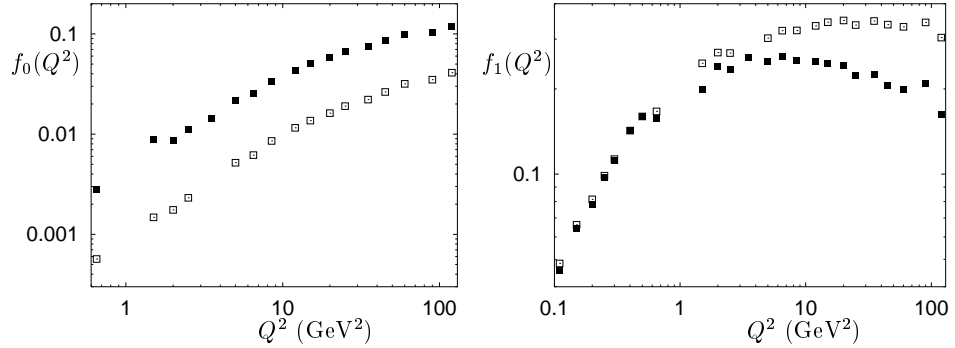


Figure 4: Fits to the coefficient functions  $f_0(Q^2)$  and  $f_1(Q^2)$  of (10) extracted from H1 and ZEUS data. The black points are for  $\epsilon_0 = 0.36$  and the white points are for  $\epsilon_0 = 0.5$ .

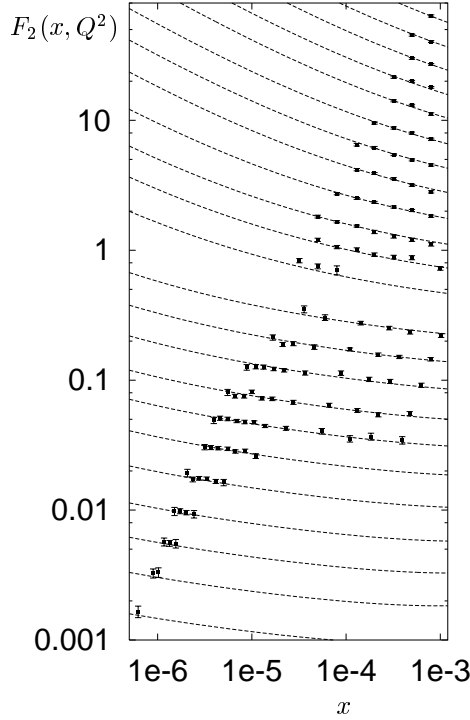


Figure 5: Regge fit to data for  $F_2(x, Q^2)$  for  $Q^2$  between 0.045 and 35  $\text{GeV}^2$

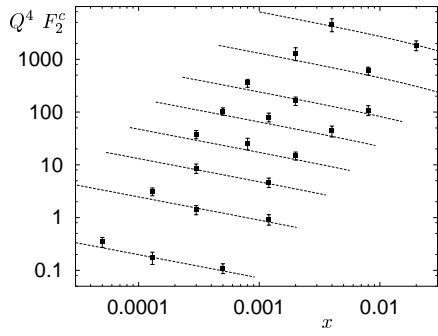


Figure 6: Data for  $F_2^c(x, Q^2)$  from  $Q^2 = 1.8$  to  $130 \text{ GeV}^2$ . The lines are the hard-pomeron component of the fit to  $F_2(x, Q^2)$  shown in figure 5, normalised such that the hard pomeron is flavour-blind.

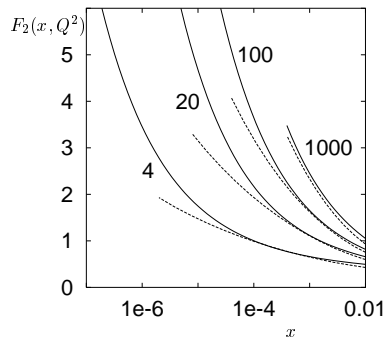


Figure 7: Two-pomeron fit to  $F_2(x, Q^2)$  at various values of  $Q^2$  (thick curves), with two-loop unresummed perturbative-QCD fit[17] (broken curves)

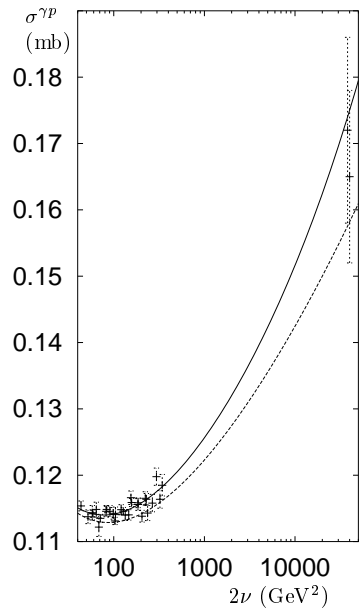


Figure 8: Data for  $\sigma^{\gamma p}$ . The upper curve is the extrapolation to  $Q^2 = 0$  of the curves in figure 5, including also a contribution from  $(f_2, a_2)$  exchange; the lower curve omits the hard-pomeron term.

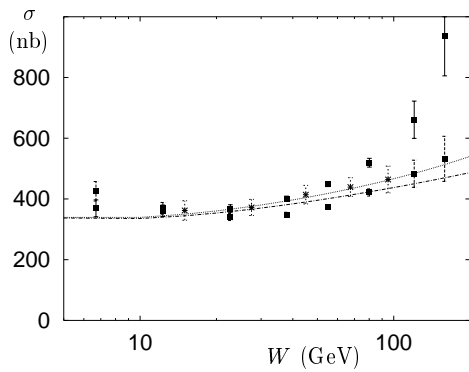


Figure 9: Data for  $\sigma^{\gamma\gamma}$ . The lower curve is the soft-pomeron/reggeon contribution; the upper curve has an additional hard-pomeron term.

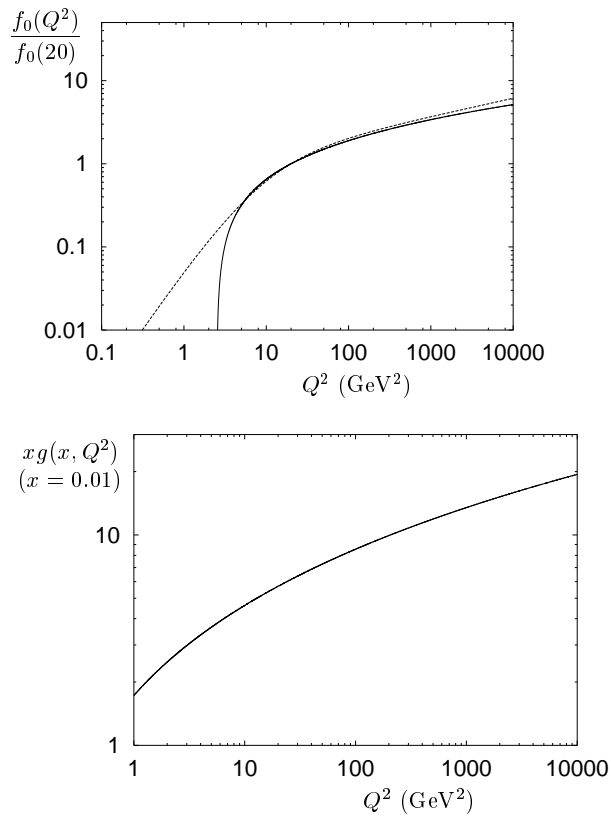


Figure 10: (a) Next-to-leading-order evolution with  $\Lambda = 400$  MeV of the hard-pomeron coefficient  $f_0(Q^2)$  (solid curve) and the fit (14) to the data (broken curve), and evolution of the gluon structure function  $xg(x, Q^2)$  at  $x = 0.01$ .

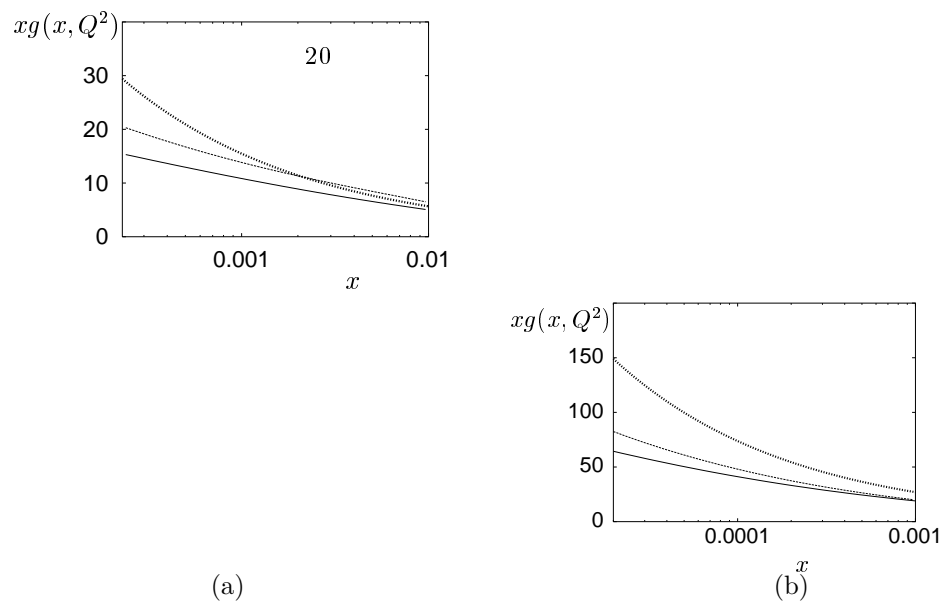


Figure 11: Gluon structure function  $xg(x, Q^2)$  at (a)  $Q^2 = 20$  and (b)  $200$  GeV $^2$ . In each case the thick line is our evolved distribution. In (a) the thin lines are the limits extracted by conventional NLO analysis of HERA data[28, 23]. In (b) the middle line is[26, 27] CTEQ5M and the lower line is[25, 27] MRST20011.